Latin American Journal of Solids and Structures
www.lajss.org

Blast Resistance of Stiffened Sandwich Panels with Closed-Cell Aluminum Foam

Abstract

In the present investigation, response of the stiffened sandwich foam panels with closed-cell aluminum foam cores subjected to blast load is examined. The panels have the metal foam sandwiched between two steel sheets. To improve resistance of the sandwich foam panel against blast, stiffeners are provided and their dynamic response under varying blast load is studied. Blast load is applied using blast equations available in LS-DYNA which takes into account reflection of blast from surface of the sandwich foam panel. Finite element based numerical simulations for dynamic analysis are performed employing a combination of shell and solid elements for steel sheets and metal foam, respectively. Quantitative assessment of dynamic response of the sandwich foam panels is made, primarily focusing on peak central point displacement of back-sheet (opposite to explosion) of the panel. Several analyses are carried out with an objective to understand the effects of stiffener configuration, foam thickness, foam density, and standoff distance on the blast response. Results indicate that the provision of stiffeners along with metal foam considerably increases blast resistance as compared to the unstiffened panels with the metal foam.

Keywords

Blast, dynamic response, metal foam, sandwich structure, steel, stiffeners.

Manmohan Dass Goel [a]
Vasant A. Matsagar [b]
Anil K. Gupta [c]

[a] Scientist, CSIR-Advanced Materials and Processes Research Institute (AMPRI), Council of Scientific and Industrial Research (CSIR), Bhopal - 462 026, India.
E-mail: mdgoel@rediffmail.com
[b] Associate Professor, Department of Civil Engineering, Indian Institute of Technology (IIT) Delhi, New Delhi - 110 016, India.
E-mail: matsagar@civil.iitd.ac.in
[c] Former Director, CSIR-Advanced Materials and Processes Research Institute (AMPRI), Council of Scientific and Industrial Research (CSIR), Bhopal - 462 026, India.
E-mail: akg51us@yahoo.co.in

Received 21.05.2014
In revised form 15.08.2014
Accepted 27.08.2014
Available online 09.10.2014

1 INTRODUCTION

Foam core sandwich panels have experienced an increased use for various applications such as sacrificial blast walls in buildings, side walls in cargo containers and boxes, and various military applications (Ashby et al., 2000). These panels possess excellent properties such as lightweight, high specific stiffness, moisture independency, and corrosion resistance. In the past, several researchers studied

blast response of the sandwich foam panels and presented the effectiveness of these panels under blast loading (Guruprasad and Mukherjee, 2000a and 2000b, Hanssen et al., 2002a and 2002b, Qiu et al., 2003, Xue and Hutchinson, 2003, Radford et al., 2006, Sriram et al., 2006, Nemat-Nasser et al., 2007, Bahei-El-Din and Dvorak, 2008, Tekalur et al., 2008, Karagiozova et al., 2009, Zhu et al., 2009, and Langdon et al., 2010). Recently, with the advancement in technology, metal foam has emerged as an important material in blast resistance applications due to their high energy absorption potential (Ashby et al., 2000). This foam has several advantages in comparison with other commonly used sandwich core materials which include (i) higher specific stiffness; (ii) lighter in weight; (iii) fire resistant; and (iv) reusability.

Most of the past research work has been carried out on the sandwich foam panels with different varieties of core ranging from fiber reinforced polymer (FRP), natural material (air, sand/soils), polymeric foams, honeycombs and commercially available metal foams (Hanssen et al., 2002a and 2002b, Qiu et al., 2003, Xue and Hutchinson, 2003, Radford et al., 2006, Sriram et al., 2006, Nemat-Nasser et al., 2007, Bahei-El-Din and Dvorak, 2008, Tekalur et al., 2008, Karagiozova et al., 2009, Zhu et al., 2009, Langdon et al., 2010, Jing et al., 2013, Chang et al., 2013, and Liu et al., 2013). No studies, however, have been reported on the stiffened sandwich foam panels and their blast response, except author's recent work on the response of stiffened polymer foam sandwich structures under impulsive loading (Goel et al., 2013a). Goel et al. (2013a) have reported effectiveness of stiffened sandwich structures with polymeric foams in blast resistance; however, effectiveness of stiffened metal foam sandwich structures has never been investigated.

In the present investigation, newly developed metal foam (Mondal et al., 2009a and 2009b) namely, closed-cell aluminum foam (ACCF) has been explored for its potential in blast applications, and its performance for blast resistance is presented. Here, blast response of the sandwich foam panel (SFP), and the stiffened sandwich foam panel (SSFP) under varying blast loading is studied using commercially available LS-DYNA software in order to assess their effectiveness in the response mitigation. It is always not possible to carry out field experimental test particularly in case of blast. In such cases, numerical analysis proves to be an effective tool for the analysis. Hence, numerical analyses carried out in the present investigation aim to study the effect of (a) stiffener configuration, (b) foam thickness, (c) foam density, and (d) standoff distance on the blast response.

2 STIFFENED SANDWICH FOAM PANEL GEOMETRY AND MATERIAL PROPERTIES

All the panels considered in present investigation have steel face- and back-sheets with ACCF as core. Back-sheet is on the opposite side of the explosion. The panels are square in shape (2 m $\times$ 2 m) with steel sheets of 10 mm thickness on each side. The back-sheet is stiffened by stiffeners of 100 mm width and 10 mm thickness for all the ten stiffened configurations with same materials (steel) as that of the face- and back-sheets. In order to investigate the effect of foam thickness on the blast response of stiffened sandwich foam panels, three foam thicknesses, 50 mm, 100 mm, and 150 mm, are considered.

Figure 1 shows various configurations of the unstiffened/stiffened sandwich foam panels considered and their nomenclature used throughout this investigation. The figure shows one unstiffened sandwich foam panel, i.e. SFP (P_1) and the stiffened sandwich foam panels with ten different stiff-

ener configurations, i.e. SSFP (P_2 to P_{11}). These configurations are arranged as per their increasing weights. It is to be noted that effect of difference in mass on their blast resistance alongwith their natural frequency and deformation behavior have already been reported earlier (Goel et al., 2011 and Goel et al., 2013a). The face-sheet and stiffened back-sheet are made of steel considering elastic-plastic and strain hardening behavior with Young's modulus, $E = 210$ GPa, Poisson's ratio, $\nu = 0.3$, and density, $\rho = 7{,}800$ kg/m^3 (Goel et al., 2011). The static yield stress of steel in the face- and back-sheets is 300 MPa. The steel face- and back-sheets along with stiffeners are modeled using elastic-plastic material model, i.e. MAT_024 (MAT_PIECEWISE_LINEAR_PLASTICITY) of LS-DYNA. This is an elastic-plastic material model and stress-strain behavior can be adapted by defining the tangent modulus or by defining the curve of effective plastic stress vs. effective plastic strain, which is equivalent to true stress vs. true strain in case of uniaxial stresses (LS-DYNA, 2011). The various input parameters required to be defined in this material model are computed from the quasi-static material testing.

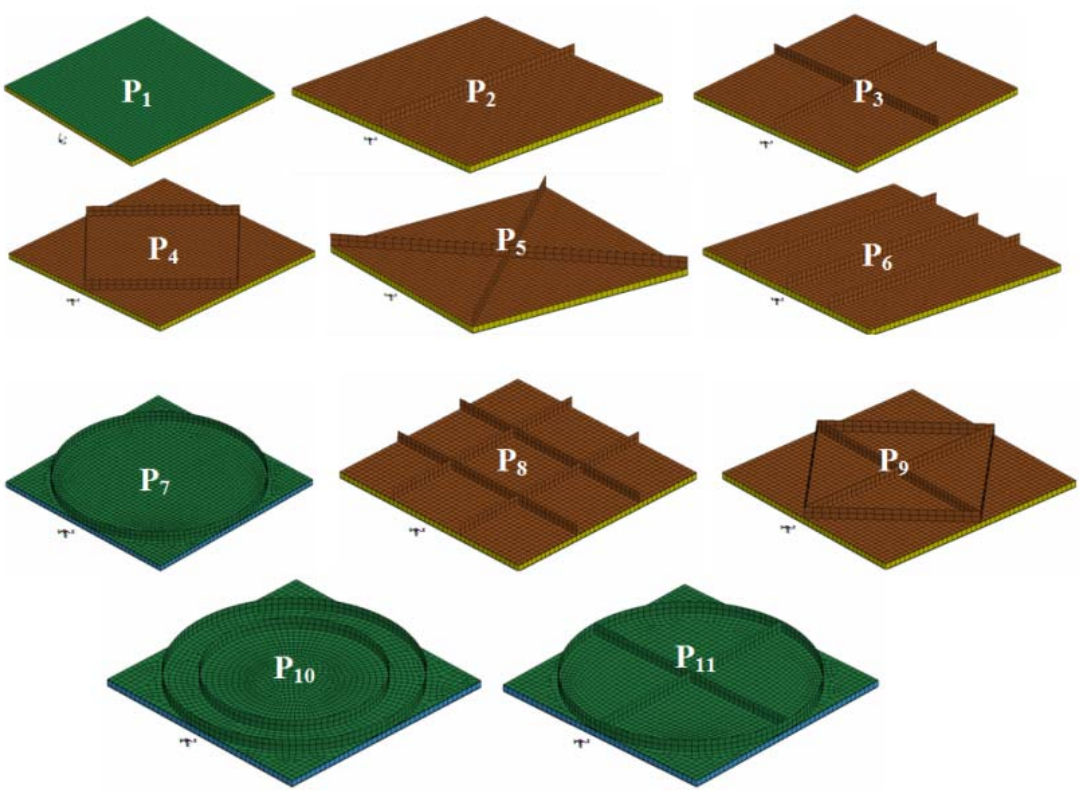

Figure 1: Sandwich foam panel configurations arranged in order of increasing weights.

Figure 2 shows the compressive stress-strain curves for three relative densities (RD) of the closed-cell aluminum foam (ACCF). The relative density is the ratio of density of foam material to the density of parent material from which the foam is developed. The patented foams are developed through liquid metallurgy route at CSIR-Advanced Materials and Processes Research Institute, Bhopal, India. Quasi-static compression tests on the aluminum foam were conducted at CSIR-

AMPRI using BiSS Universal Testing Machine (Model Bi-00-002, 50 kN Load Cell) at a strain rate of 0.001/s. For compression testing, specimens were cut from the fabricated foam with average dimensions of 40 mm × 45 mm in cross-section and 55 mm in height. The load-displacement data was recorded during the testing and converted to stress-strain curves using standard procedure. The mechanical behavior of these foam materials is reported elsewhere in details (Mondal et al., 2009a and 2009b, and Goel et al., 2013b). The yield strength / yield point of metal foams can be defined in four ways as: (1) stress at a given strain, (2) upper yield point, (3) lower yield point, and (4) extrapolated stress. In the present investigation, yield strength / yield point is considered as upper yield point as shown in Figure 2. Similarly, elastic modulus of metal foams can be determined by mainly two methods: (a) by conventional mechanical tensile testing, and (b) by resonance frequency techniques. Herein, the resonance frequency technique is employed for determination of elastic modulus (Mondal et al., 2009a and 2009b). It is to be noted that this foam has closed cell structure which is considered superior in energy absorption applications as compared to the open cell foam (Ashby et al., 2000).

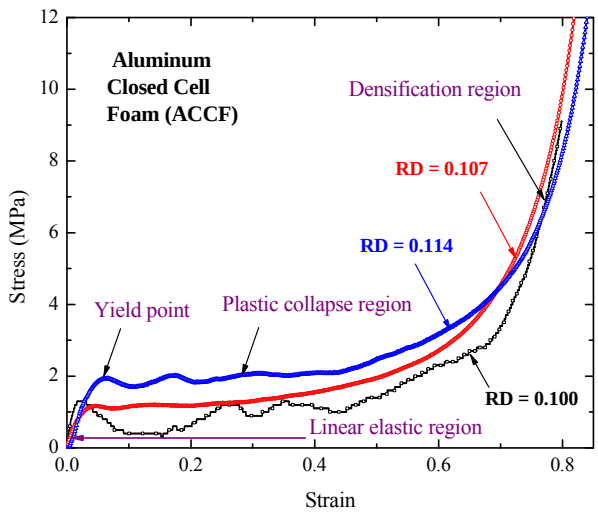

Figure 2: Compressive stress-strain curves for closed-cell aluminum foam.

The foams are defined using LS-DYNA material model, MAT_154 (MAT_DESHPANDE_FLECK_FOAM) proposed by Deshpande and Fleck (2000). Following Deshpande-Fleck foam model, yield stress function (Φ) of foam material is defined as, $\Phi = \sigma_e - \sigma_y$, where, σ_y is the yield stress of foam material and σ_e is the equivalent stress defined as, $\sigma_e^2 = \dfrac{\sigma_{VM}^2 + \alpha^2\sigma_m^2}{1+(\alpha/3)^2}$. In this expression, σ_{VM} is the von-Mises stress and σ_m is the mean stress. The shape of yield surface is controlled by the shape parameter, α. The yield stress is governed by the model presented by Hanssen et al. (2002a and 2002b) as,

$$\sigma_y = \sigma_p + \lambda\frac{e}{e_D} + \alpha_2 \ln\left[\frac{1}{1-(e/e_D)^\beta}\right] \tag{1}$$

where, e is engineering strain; σ_p is plateau stress; λ, α_2, and β are material parameters; and e_D is the foam densification strain expressed in terms of density of the foam (ρ_f) and density of the parent material (ρ_0) as,

$$e_D = -\ln\left(\frac{\rho_f}{\rho_0}\right) \tag{2}$$

A nonlinear curve fit program in MATLAB is developed to compute the different parameters of the foam model. Table 1 shows various mechanical properties obtained using the MATLAB non-linear curve fit program for the foam used in the present investigation.

Type of Foam	**RD**	***E*** **(GPa)**	**λ** **(MPa)**	**α_2** **(MPa)**	**β**	**σ_p** **(MPa)**
Closed-cell aluminum foam (ACCF)	0.100	1.1	0.0253	1.605	2.17	0.77
	0.107	1.2	0.202	2.086	2.14	1.17
	0.114	1.3	0.861	1.27	2.18	1.71

Table 1: Foam material properties.

3 FINITE ELEMENT MODELS AND BLAST LOADING

Finite element (FE) models of the sandwich foam panels are developed using Box_Solid feature available in LS-DYNA. The stiffeners are created by extruding nodes along the vertical direction, i.e. direction perpendicular to the back-sheet, and assigning the surface to create geometry of the back-sheets in HYPERMESH (ALTAIR, 2007). The foam is modeled as solid elements whereas, face- and back-sheets in conjunction with stiffeners are modeled using shell elements. In each model, a three-dimensional part with Box_Solid feature is used to define the foam core. Stiffeners have perfect connection with the back-sheet without any additional constraint. Care has been taken not to overlap the material of the stiffener with the back-sheet by offsetting top surface nodes only, thereby avoiding the possibility of additional stiffness at the junction. Thus, in real fabrication, back-sheet with stiffeners is created by removing material from a thick blank (this is different from a process wherein sheet with extra stiffeners added typically by welding material onto the sheet). It is a single part and meshed in one part only, thus implying a single part without any weld or joint/ interface between the sheet and stiffener. Geometry of sheets and stiffeners are modeled using Belytschko-Tsay shell elements available in the LS-DYNA element library, whereas eight-node solid elements with full integration are used along with hourglass control to model the geometry of the foam core (LS-DYNA, 2011). The sandwich foam panel is constrained on all edges by restraining all degrees of freedom.

4 BLAST LOADING

The blast load in the present investigation is applied on face-sheet of the sandwich foam panels using blast function (LOAD_BLAST_ENHANCED) available in LS-DYNA with CONWEP (CONWEP, 1991). This formulation takes into account pressure enhancement due to reflection of blast from the surface of sandwich foam panels and is analyzed for three different standoff distances, i.e. 1.5 m, 2.0 m, and 2.5 m. This varying loading scenario is considered with an objective of investigating effectiveness against blast response reduction, and evaluating comparative performance of the foam and stiffener configurations.

Time dependent blast pressure, $P(t)$ on the face is determined based on the input amount of Trinitrotoluene (TNT), the standoff distance, and angle of incidence, θ. Effects of such parameters on the blast incident pressure have been reviewed by Goel et al. (2012). The blast pressure is computed using following equation in LS-DYNA,

$$P(t) = P_r \cos^2\theta + P_i\left(1 + \cos^2\theta - 2\cos\theta\right) \tag{3}$$

where, P_r and P_i are the reflected and incident pressures, respectively. Computation of P_r and P_i is reported in details elsewhere (Goel et al., 2012). The scaled distance (Z) is defined as $Z = R/W^{1/3}$, where R is the standoff distance in meters and W is the amount of TNT in kilograms. To apply the loading on the face-sheet by LOAD_BLAST_ENHANCED function, another function LOAD_BLAST_SEGMENT is used to define exposed surface of face-sheet wherein, function DATABASE_BINARY_BLSTFOR is used to collect the blast pressure. The calculated loading is presented in Figure 3 for three different standoff distances considered. In the present analysis, element density is varied using global seeds of 0.01, 0.05, and 0.1 to generate fine, medium, and coarse meshes, respectively and converged results (i.e. finite element mesh with global seed of 0.05) are only presented. Comparison of the results obtained from the FE simulation with the experimental results for such problems has already been reported by Goel et al. (2011 and 2013a).

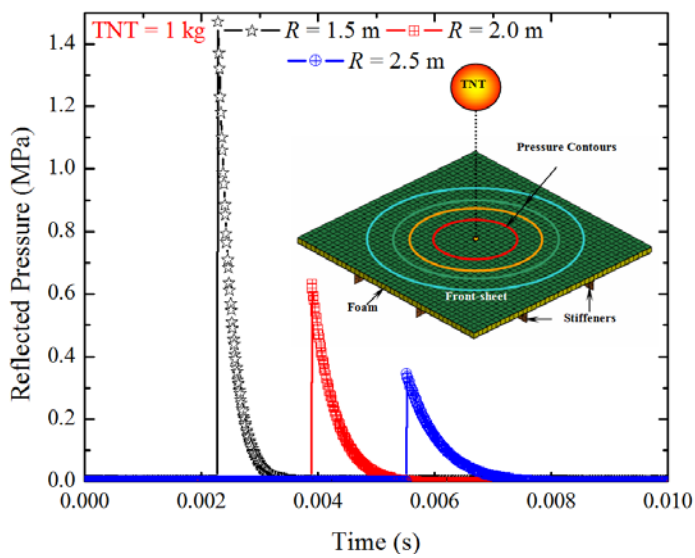

Figure 3: Blast pressure time histories for three standoff distances.

5 RESULTS AND DISCUSSION

Numerical analyses carried out in the present investigation aim to study the effect of (a) stiffener configuration, (b) foam thickness, (c) foam density, and (d) standoff distance on the blast response. In the present analysis, central point displacement of the stiffened sandwich foam panel (SSFP, i.e. P_2 to P_{11}) is compared with the sandwich foam panel (SFP, i.e. P_1) designated as base model (referenced as 100% weight). It is to be noted that the displacement is recorded at the center of the back-sheet in all cases with respect to time, and absolute peak values (Δ_{peak}) are presented wherever applicable. The measure of effectiveness of the sandwich foam panel is quantified using central point displacement; such that lower the central point displacement higher the effectiveness.

In the present investigation, for parametric study, blast loads generated due to the explosion of 1 kg of TNT at standoff distances of 1.5 m, 2.0 m, and 2.5 m are considered. The peak pressures resulting due to this combination of TNT and standoff distances are shown in Figure 3. The face-sheet of the panels is exposed to blast and the TNT is placed exactly at the centre maintaining the considered standoff distances of the panels (Figure 3). Three different relative densities (RD) of the foam (0.100, 0.107, and 0.114) are used for core material, as reported in Table 1.
Figure 4 shows the central point displacement time histories of the SSFP-ACCF panels for three thicknesses of the foam core (t_f = 50, 100, and 150 mm), for a foam relative density of 0.100 and standoff distance of 1.5 m subjected to the blast loading. Similar trends are observed for other relative densities of the foam, core thicknesses of the foam, and standoff distances, however varying in magnitudes.

In order to compare the results of peak central point displacement for the SSFP-ACCF and to understand the effect of relative densities, core thicknesses of the foam and standoff distances, common plots for a representative foam thickness (50 mm) are reported in Figure 5. The peak central point displacements for all the combinations of density, foam thickness, and standoff distances are reported in Table 2 through Table 4. Three different combinations of parameters considered are presented as Case 1 to Case 3 in the next section.

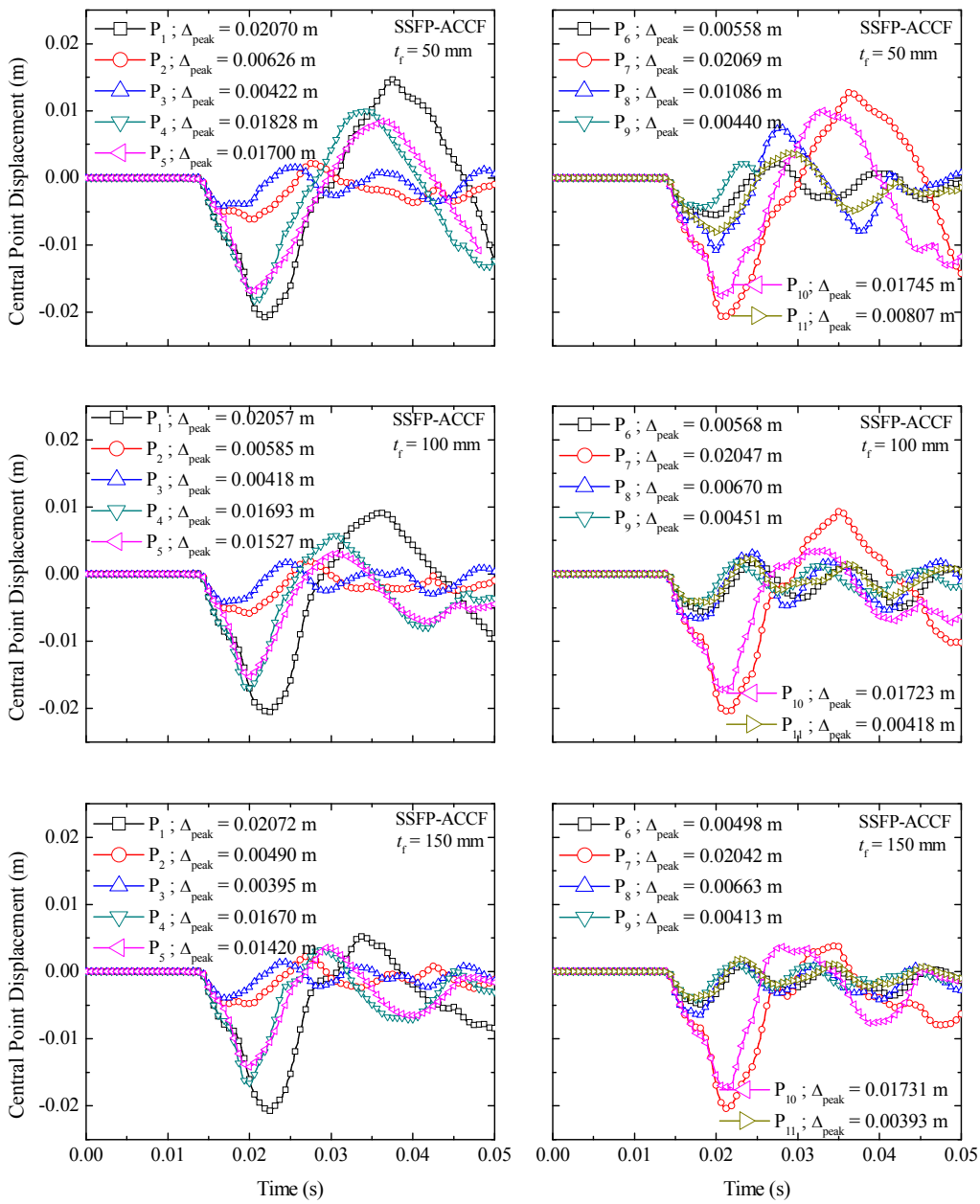

Figure 4: Central point displacement time histories of SSF- and SSFP-ACCF for three foam thicknesses, $t_f = 50$, 100, and 150 mm for foam RD = 0.100 and $R = 1.5$ m.

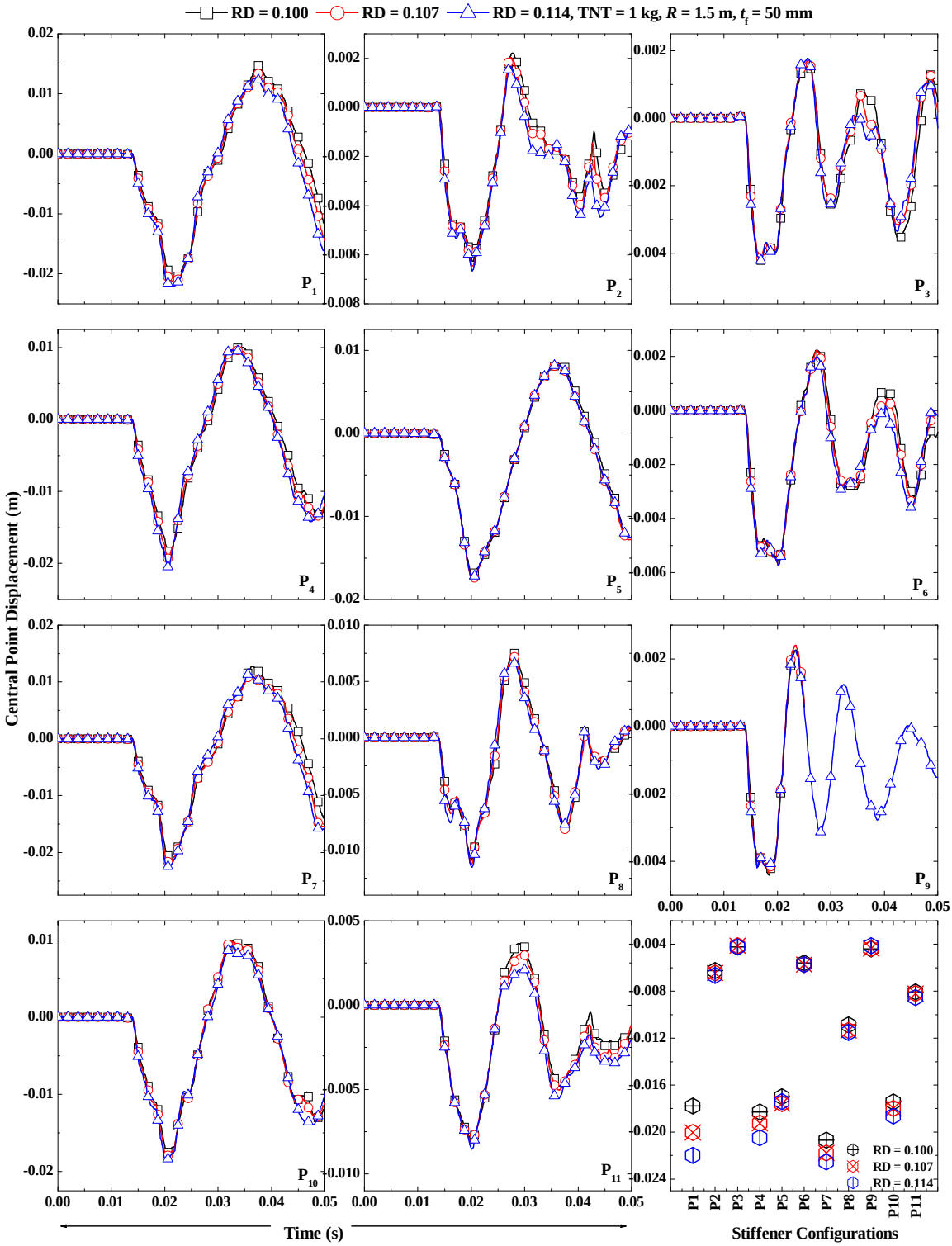

Figure 5: Central point displacement time histories of SSF- and SSFP-ACCF for foam thickness, $t_f = 50$ mm for foam RD = 0.100, 0.107, 0.114, $R = 1.5$ m and TNT =1 kg.

Case 1: Sandwich foam panels with 50, 100, and 150 mm thick foam core with 1 kg TNT and 1.5 m standoff distance

Comparison of peak central point displacements of the sandwich foam panels with different relative densities for 50 mm thick foam core show that the panels with foam relative density of 0.100 results in lowest peak central point displacement for all the panel configurations (except P_3 and P_9) as compared to the panels with foam core relative densities of 0.107 and 0.114 for the same level of blast loading (Table 2 and Figure 4). The lowest central point displacement (i.e. 4.13 mm) for 50 mm thick foam core is observed for the panel configuration P_9 with RD = 0.114 (Table 2). However, the panel configuration P_{11} with RD = 0.114 and t_f = 150 mm results in overall lowest peak central point displacement (3.67 mm) for 1.5 m standoff distance (Table 2). This may be attributed to the fact that higher foam thickness available in these configurations result in lower impulse transfer to the back-sheet. It can further be noted that the introduction of foam results in higher response reduction except configuration P_7 for all the relative densities of foam and configuration P_4 for RD = 0.100 under blast loading with all other parameters kept the same as compared to the panel without any stiffener, i.e. P_1. The reason for higher peak displacement in case of the panels P_4 and P_7 is attributed to the fact that stiffeners in these configurations do not pass through the centre point of the panels resulting in localized response. Similar observations are made for the foam core thicknesses of 100 and 150 mm for P_7, whereas configuration P_4 results in lower peak central point displacement as compared to P_1. However, in case of P_1 configuration, increasing foam relative density results in enhancement of peak central point displacement with the higher thickness of foam core. Further, improved performance of the low density foam with lowest foam thickness is achieved because the low density foam hardens at low stress levels than those with higher density foams for the same level of blast loading (Figure 2).

Panels Nomenclature	Peak Central Point Displacement (m) , Δ_{peak}					
	Stiffened Sandwich Foam Panel (SSFP)					
	ACCF, RD = 0.107, R = 1.5 m			ACCF, RD = 0.114, R = 1.5 m		
	t_f = 50 mm	t_f = 100 mm	t_f = 150 mm	t_f = 50 mm	t_f = 100 mm	t_f = 150 mm
P_1 (SFP)	0.02003	0.02142	0.02215	0.02200	0.02215	0.02290
P_2	0.00646	0.00585	0.00585	0.00666	0.00585	0.00523
P_3	0.00413	0.00417	0.00399	0.00421	0.00399	0.00368
P_4	0.01926	0.01853	0.01979	0.02047	0.01979	0.01920
P_5	0.01757	0.01552	0.01590	0.01739	0.01590	0.01592
P_6	0.00572	0.00542	0.00505	0.00574	0.00505	0.00490
P_7	0.02177	0.02193	0.02314	0.02253	0.02314	0.02368
P_8	0.01133	0.00690	0.00683	0.01153	0.00683	0.00683
P_9	0.00435	0.00434	0.00421	0.00413	0.00421	0.00369
P_{10}	0.01797	0.01803	0.01882	0.01862	0.01882	0.02004
P_{11}	0.00821	0.00413	0.00399	0.00853	0.00399	0.00367

Table 2: Peak central point displacements for SFP- and SSFP-ACCF for different thicknesses and R = 1.5 m.

Case 2: Sandwich foam panels with 50, 100, and 150 mm thick foam core with 1 kg TNT and 2 m standoff distance

Comparison of peak central point displacements of the sandwich foam panels with 50, 100, and 150 mm thick foam core with different relative densities show that the panels with foam relative density of 0.100 results in lowest peak central point displacement for all the panel configurations for the same level of blast loading (Figure 4). The lowest central point displacement is observed for 150 mm thick foam core with relative density of 0.100 for the panel configuration P_{11} (3.05 mm) for 2 m standoff distance (Table 3 and Figure 4).

Panels Nomenclature	**Peak Central Point Displacement (m) , Δ_{peak}**					
	Stiffened Sandwich Foam Panel (SSFP)					
	ACCF, RD = 0.107, R = 2 m			**ACCF, RD = 0.114, R = 2 m**		
	t_f = 50 mm	**t_f = 100 mm**	**t_f = 150 mm**	**t_f = 50 mm**	**t_f = 100 mm**	**t_f = 150 mm**
P_1 (SFP)	0.01596	0.02007	0.02008	0.01953	0.02109	0.02081
P_2	0.00443	0.00431	0.00378	0.00464	0.00448	0.00385
P_3	0.00328	0.00329	0.00316	0.00339	0.00340	0.00320
P_4	0.01558	0.01607	0.01457	0.01618	0.01677	0.01478
P_5	0.01308	0.01163	0.01147	0.01299	0.01220	0.01188
P_6	0.00431	0.00450	0.00441	0.00441	0.00462	0.00440
P_7	0.01836	0.01973	0.01924	0.01957	0.02057	0.01978
P_8	0.00823	0.00626	0.00620	0.00852	0.00621	0.00624
P_9	0.00356	0.00371	0.00360	0.00340	0.00377	0.00371
P_{10}	0.01360	0.01510	0.01549	0.01458	0.01597	0.01566
P_{11}	0.00664	0.00327	0.00311	0.00708	0.00337	0.00374

Table 3: Peak central point displacements for SFP- and SSFP-ACCF for different thicknesses and R = 2 m.

It can be further noted that the introduction of foam results in higher response reduction except for configuration P_7 (50 mm thick foam core) for all foam relative densities however, excluding foam relative density of 0.114 and 150 mm thick foam. The peak displacement of P_7 configuration with t_f = 150 mm is 19.78 mm whereas the peak displacement of P_1 configuration is 20.81 mm for the same level of blast loading (Table 3). The reason for higher peak displacement in case of the panel P_7 is attributed to the fact that stiffeners in this configuration do not pass through the centre point of the panel, i.e. peak displacement point.

The peak central point displacements of panels for this combination of loading exhibit varied trends for all the thicknesses of the foam core. Again, the maximum displacement is observed for the unstiffened panel configuration and all other configurations show lower peak central point displacement indicating the effectiveness of using closed-cell aluminum foam with suitable stiffener configuration for a particular thickness of the foam core.

Case 3: Sandwich foam panels with 50, 100, and 150 mm thick foam core with 1 kg TNT and 2.5 m standoff distance

The peak central point displacements of panels in this scenario of loading results in similar trend as observed for Case 2. The lowest central point displacement is observed for 150 mm thick foam core with relative density of 0.100 for the panel configuration P_{11} (2.45 mm) for 2.5 m standoff distance (Table 4 and Figure 4).

It can be further noted that the introduction of foam results in higher response reduction except for configuration P_7 (50 mm thick foam core) for all the relative densities of the foam. The panel configuration P_7, however, results in higher peak displacement as compared to that of the P_1 configuration with 50 mm thick foam for the same level of blast loading, for the same reason as mentioned above that the stiffeners do not pass through the centre point of the panel.
The peak central point displacements of panels for this combination of loading exhibit varied trends for all the thicknesses of the foam core. Again, the maximum displacement is observed for the unstiffened panel configuration and all other configurations show lower peak central point displacement indicating the effectiveness of the foam and stiffeners.

Panels Nomenclature	Peak Central Point Displacement (m), Δ_{peak}					
	Stiffened Sandwich Foam Panel (SSFP)					
	ACCF, RD = 0.107, R = 2.5 m			ACCF, RD = 0.114, R = 2.5 m		
	t_f = 50 mm	t_f = 100 mm	t_f = 150 mm	t_f = 50 mm	t_f = 100 mm	t_f = 150 mm
P_1 (SFP)	0.01326	0.01820	0.01838	0.01867	0.01923	0.01946
P_2	0.00357	0.00334	0.00308	0.00299	0.00351	0.00336
P_3	0.00281	0.00278	0.00267	0.00421	0.00300	0.00284
P_4	0.01438	0.01376	0.01311	0.01532	0.01450	0.01370
P_5	0.01113	0.01027	0.00977	0.01098	0.01075	0.01015
P_6	0.00343	0.00367	0.00347	0.00353	0.00379	0.00370
P_7	0.01775	0.01807	0.01745	0.01907	0.01902	0.01849
P_8	0.00778	0.00508	0.00539	0.00813	0.00504	0.00577
P_9	0.00311	0.00323	0.00310	0.00328	0.00345	0.00330
P_{10}	0.01336	0.01403	0.01382	0.01429	0.01482	0.01459
P_{11}	0.00581	0.00278	0.00260	0.00630	0.00299	0.00284

Table 4: Peak central point displacements for SFP- and SSFP-ACCF for different thicknesses and R = 2.5 m

Parametric Study

In order to understand the effects of various parameters on blast response of the panels, the peak central point displacements of all the panel configurations are presented in Figure 6, with varying standoff distances, foam densities, and foam thicknesses.

5.1 Effect of stiffener configurations

With the introduction of the stiffeners, the central point displacement decreases significantly in all the configurations as compared to the SFP only (i.e. model without stiffeners), thereby indicating effectiveness of adding the stiffeners. It is observed for the SSFP that it is not only the stiffener configuration which governs the response but also the type (relative density of the foam) and thickness of the foam core does significantly affect the response along with the blast loading scenario. Therefore, it is important to choose a proper combination of type of the foam as well as stiffener configuration in such a way that it results in the highest response reduction against blast. From Figure 6, it is concluded that the panels with circular stiffener configurations (P_7, P_{10}, and P_{11}) exhibit lower response reduction as compared to the panels with rectangular stiffener configurations. It is found that introduction of foam results in higher response reduction except for the panel with circular configuration for all the relative densities of foam and the panel with rhombus configuration (i.e. P_4) for 0.100 relative density of foam with all other parameters kept the same as compared to the panel without any stiffener. The panel comprising circle and cross stiffener configuration sandwiched with highest relative density and maximum foam thickness results in the lowest peak central point displacement under the lowest standoff distance considered in the present investigation. Moreover, it can be noted that for achieving improved blast response reduction, the provided stiffener should pass through the region experiencing higher deflection and reach the panel boundaries with all other parameters kept the same. Thus, this study confirms that several numerical simulations indeed help in selecting the foam and stiffener types through finite element (FE) modeling which in turn reduces the experimental work not only in terms of efforts but also in saving considerable time and resources, particularly under blast loadings.

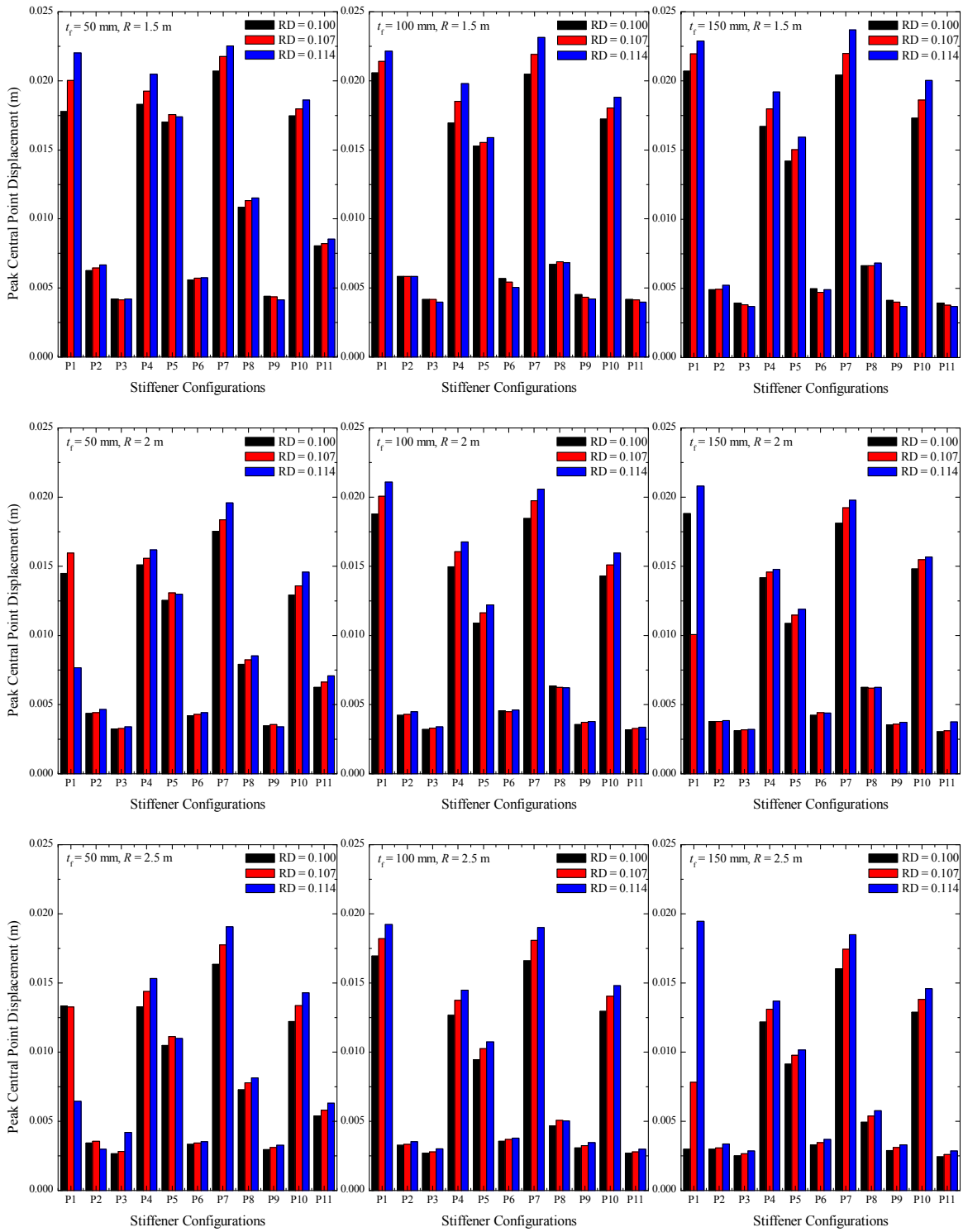

Figure 6: Central point displacement time histories of SSF- and SSFP-ACCF for foam thickness, $t_f = 50$, 100, 150 mm for foam RD = 0.100, 0.107, 0.114 and $R = 1.5$, 2.0, 2.5 m.

5.2 Effect of foam thickness

From Figure 6 it is observed that the central point displacement decreases with the increase in the foam core thickness for the ACCF. This is evident because of higher energy dissipation and increased stiffness of the core. Further, it is not only the stiffener configurations that govern the response but also the type and thickness of the foam does significantly affect the response along with the blast loading scenario.

5.3 Effect of foam relative density

It is evident from the trends observed in Figure 6 that the higher density of foam core results in higher peak central point displacements. Further, it is found that panels with least foam relative density results in lowest peak central point displacement for all the panel configurations (except for P_3 and P_9) as compared to the panels with other foam core relative densities for the same level of blast loading. Moreover, it is observed that lowest central point displacement for 50 mm thick foam core for the panel configuration P_9 with highest foam relative density for least standoff distance considered in the present investigation. From this study, it is observed that lowest density foam largely performs better with lowest foam thickness in comparison with higher foam densities and thicknesses for least standoff distance considered in the present investigation.

5.4 Energy balance study

In order to gain an insight of response mitigation, energy studies for all the panels are carried out. The time histories of energy help in identifying and highlighting the significant physical effects caused due to impulsive loading on the panels. The total energy of the FE models has been checked for hourglass energy and is found to be insignificant indicating the nonexistence of hourglass effect. The total energy imparted by the applied impulsive loading to the sandwich foam panels is converted to kinetic and internal energies. The internal energy is dissipated in inelastic deformation in the material parts. The internal and kinetic energies of the sandwich foam panels are shown respectively in Figure 7 and Figure 8 for SSF- and SSF-ACCF, three foam thicknesses for a foam RD = 0.100 with $R = 1.5$ m. It is observed that at the end of the blast load, the panels vibrate freely with increase in the kinetic energy. When the panel is at its maximum deflection, it has maximum internal energy and minimum kinetic energy. From the plots of the kinetic energy, it is evident that the second rise in the internal energy occurs when the panel rebounds from its maximum displacement and it moves back in the opposite direction. The total internal energy of the SFP is higher than that of the SSFP and so is the kinetic energy for types of foams and all the stiffener configurations considered herein. Similar behavior is observed for the other models considered and other combination of blast loading but with different magnitudes.

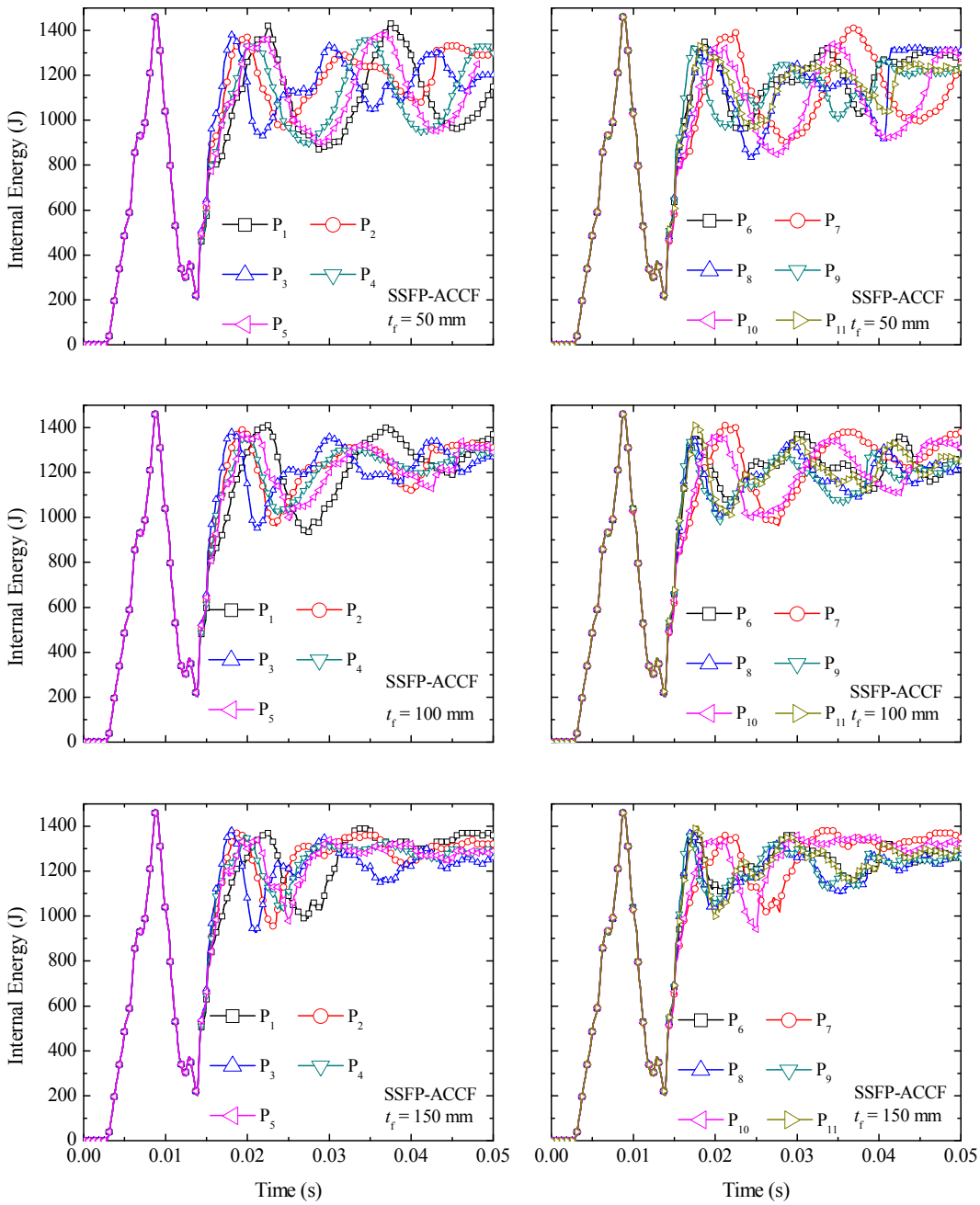

Figure 7: Internal energies for SSF- and SSF-ACCF, $t_f = 50$, 100, and 150 mm, foam RD = 0.100, $R = 1.5$ m.

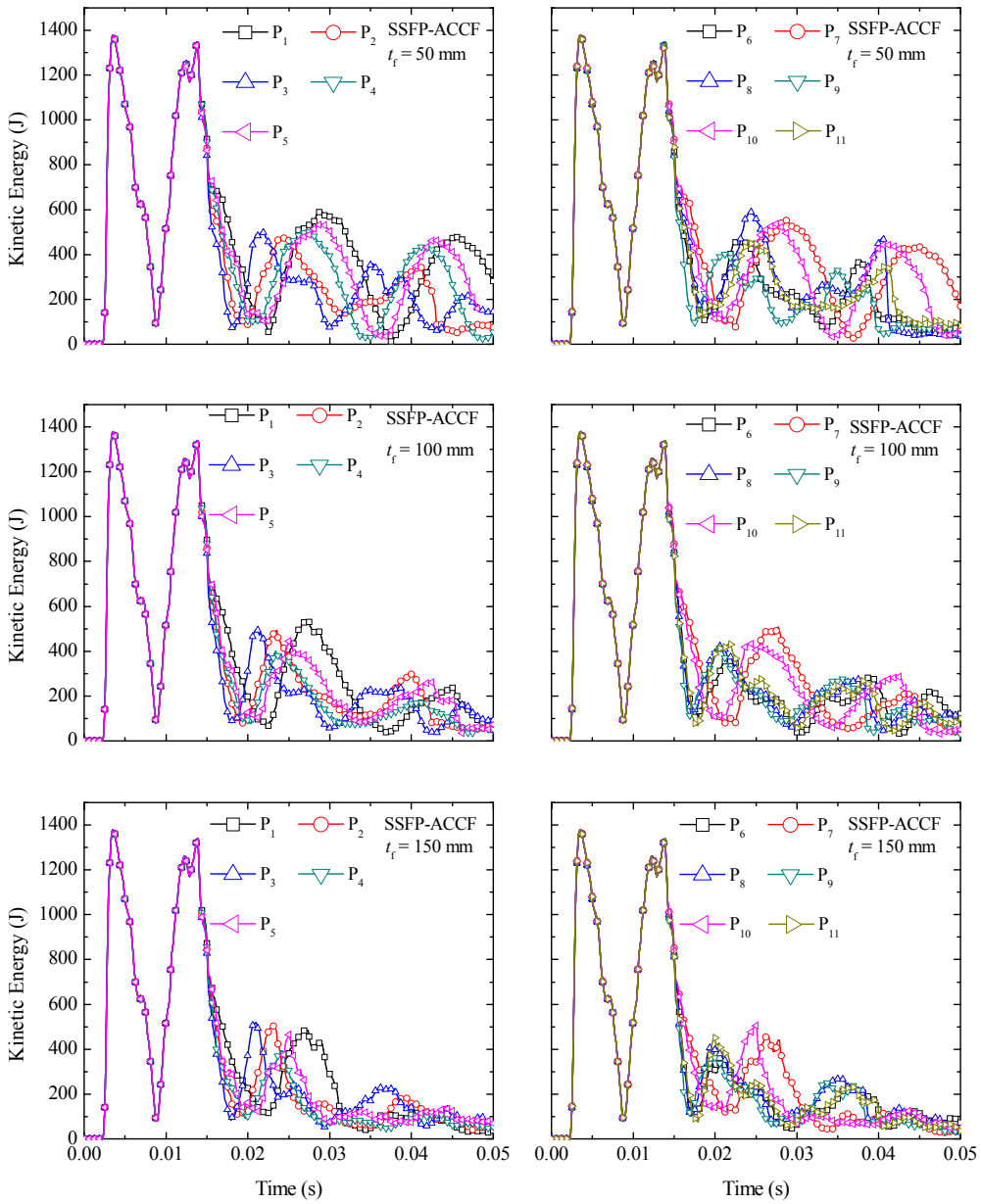

Figure 8: Kinetic energies for SSF- and SSF-ACCF, $t_f = 50$, 100, and 150 mm, foam RD = 0.100, $R = 1.5$ m.

6 CONCLUSIONS

Response of the sandwich foam panels subjected to varying blast loading is presented to study the effect of (a) stiffener configuration, (b) foam thickness, (c) foam density, and (d) standoff distance on the blast response. The following conclusions are drawn from the present study:

1. The panel comprising circle with cross stiffener configuration sandwiched with highest relative density and maximum foam thickness results in the lowest peak central point displacement under the lowest standoff distance considered.
2. Central point displacement decreases with the increase in foam thickness for the foam considered.
3. Introduction of foam results in higher response reduction except for the panel with circular configuration.
4. Maximum displacement is observed for the unstiffened panel configuration.
5. Lowest density foam largely performs better with lowest foam thickness in comparison with higher foam densities and thicknesses for least standoff distance considered in the present investigation.
6. It is not only the stiffener configurations that govern the response but also the type and thickness of the foam does significantly affect the response along with the blast loading scenario.
7. The total internal energy of the unstiffened sandwich foam panel is higher than that of the stiffened sandwich foam panel and so is the kinetic energy for both the types of foams and all the stiffener configurations considered in the present investigation.

References

ALTAIR (2007). User Manual. Altair Engineering Corporation, U.S.A.

Ashby, M.F., Evans, A.G. and Fleck, N.A., (2000). Metal Foams: A Design Guide, Butterworth Heinmann, Oxford, U.K.

Bahei-El-Din, Y.A. and Dvorak, G.J., (2008). Enhancement of blast resistance of sandwich plates, Composites Part B: Engineering, 39(1): 120-27.

Chang, Q., Shu, Y., Li-Jun, Y., Zhi-Yong, W., Zhen-Hua, L., (2013). Blast resistance and multi-objective optimization of aluminum foam-cored sandwich panels, Composite Structures, 105: 45-57.

CONWEP (1991). Conventional Weapons Effects Program, Version 2.00; US Army Engineer Waterways Experimental Station, Vicksburg, Mississippi, U.S.A.

Deshpande, V.S. and Fleck, N.A., (2000). Isotropic constitutive models for metallic foams, Journal of the Mechanics and Physics of Solids, 48(6): 1253-83.

Goel, M.D., Matsagar, V.A., Gupta, A.K., (2011). Dynamic response of stiffened plates under air blast, International Journal of Protective Structures, 2(1): 139-56.

Goel, M.D., Matsagar, V.A., Gupta, A.K., Marburg, S., (2012). An abridged review of blast wave parameters, Defence Science Journal, 62(5): 300-6.

Goel, M.D., Matsagar, V.A., Marburg, S., Gupta, A.K., (2013a). Comparative performance of stiffened sandwich foam panels under impulsive loading, Journal of Performance of Constructed Facilities, ASCE, 27(5): 540-49.

Goel, M.D., Matsagar, V.A., Gupta, A.K., Marburg, S., (2013b). Strain rate sensitivity of closed cell aluminum fly ash foam, Transactions of Nonferrous Metals Society of China, 23: 1080-89.

Guruprasad, S. and Mukherjee, A., (2000a). Layered sacrificial claddings under blast loading part-I analytical studies, International Journal of Impact Engineering, 24(9): 957-73.

Guruprasad, S. and Mukherjee, A., (2000b). Layered sacrificial claddings under blast loading part-II experimental studies, International Journal of Impact Engineering, 24(9): 975-84.

Hanssen, A.G., Enstock, L., Langseth, M., (2002a). Close-range blast loading of aluminum foam panels, International Journal of Impact Engineering, 27(6): 593-618.

Hanssen, A.G., Hopperstad, O.S., Langseth, M., Ilstad, H., (2002b). Validation of constitutive models applicable to aluminum foams, International Journal of Mechanical Sciences, 44: 359-406.

Jing, L., Yang, F., Wang, Z., Zhao, L., (2013). A numerical simulation of metallic cylindrical sandwich shell subjected to air blast loading, Latin American Journal of Solids and Structures, 10: 631-45.

Karagiozova, D., Nurick, G.N., Langdon, G.S., Yuen, S.C.K., Chi, Y., Bartle, S., (2009). Response of flexible sandwich-type panels to blast loading, Composites Science and Technology, 69(6): 754-63.

Langdon, G.S., Nurick, G.N., Yahya, M.Y., Cantwell, W.J., (2010). The response of honeycomb core sandwich panels with aluminum and composite face sheets to blast loading, Journal of Sandwich Structures and Materials, 12(6): 733-54.

Liu, H., Cao, Z.K., Yao, G.C., Luo, H.J., Zu, G.Y., (2013). Performance of aluminum foam–steel panel sandwich composites subjected to blast loading, Materials and Design, 47: 483-88.

LS-DYNA (2011). Theory Manual, Livermore Software Technology Corporation, Livermore, California, U.S.A.

Mondal, D.P., Goel, M.D., Das, S., (2009a). Compressive deformation and energy absorption characteristics of closed cell aluminium-fly ash particle composite foam, Materials Science and Engineering: A, 507(1-2): 102-9.

Mondal, D.P., Goel, M.D., Das, S., (2009b). Effect of strain rate and relative density on compressive deformation behavior of closed cell aluminum-fly ash composite foam, Materials and Design, 30(4): 1268-74.

Nemat-Nasser, S., Kang, W.J., McGee, J.D., Guo, W.-G., Isaacs, J.B., (2007). Experimental investigation of energy-absorption characteristics of components of sandwich structures, International Journal of Impact Engineering, 34(6): 1119-46.

Qiu, X., Deshpande, V.S., Fleck, N.A., (2003). Finite element analysis of the dynamic response of clamped sandwich beams subject to shock loading, European Journal of Mechanics - A/Solids, 22(6): 801-14.

Radford, D.D., McShane, G.J., Deshpande, V.S., Fleck, N.A., (2006). The response of clamped sandwich plates with metallic foam cores to simulated blast loading, International Journal of Solids and Structures, 43(7-8): 2243-59.

Sriram, R., Vaidya, U.K., Kim, J.-E., (2006). Blast impact response of aluminum foam sandwich composites, Journal of Materials Science, 41(13): 4023-39.

Tekalur, S.A., Shukla, A., Shivakumar, K., (2008). Blast resistance of polyuria based layered composite materials, Composite Structures, 84(3): 271-81.

Xue, Z. and Hutchinson, J.W., (2003). Preliminary assessment of sandwich plates subject to blast loads, International Journal of Mechanical Sciences, 45(4): 687-705.

Zhu, F., Zhao, L., Lu, G., Gad, E., (2009). A numerical simulation of the blast impact of square metallic sandwich panels, International Journal of Impact Engineering, 36(5): 687-99.